

Full Length Article

Carbon nanosphere templates for the preparation of inverse opal titania photonic crystals by atomic layer deposition

László Péter Bakos^{a,*}, Dániel Karajz^a, András Katona^a, Klara Hernadi^b, Bence Párditka^c, Zoltán Erdélyi^c, István Lukács^d, Zoltán Hórvölgyi^e, Géza Sztási^f, Imre Miklós Szilágyi^a

^a Department of Inorganic and Analytical Chemistry, Budapest University of Technology and Economics, Szent Gellért tér 4, H-1111 Budapest, Hungary

^b Department of Applied and Environmental Chemistry, University of Szeged, Rerrich Béla tér 1, H-6720 Szeged, Hungary

^c Department of Solid State Physics, Faculty of Sciences and Technology, University of Debrecen, P.O. Box 400, H-4002 Debrecen, Hungary

^d Hungarian Academy of Sciences, Research Centre for Energy, Institute of Technical Physics and Materials Science, Konkoly Thege M. út 29-33, H-1121 Budapest, Hungary

^e Department of Physical Chemistry and Materials Science, Budapest University of Technology and Economics, Budaörsi út 8. F. I. Building, H-1111 Budapest, Hungary

^f Femtonics Ltd, Tízoltó utca 59, H-1094 Budapest, Hungary

ARTICLE INFO

Keywords:

Carbon nanospheres

TiO₂

Inverse opal photonic crystal

Photocatalysis

ABSTRACT

Carbon nanospheres were used as templates for the first time to prepare titania inverse opal photonic crystal. From the spheres, opal colloid crystals were made by vertical deposition on microscope slides, and TiO₂ was grown on them using atomic layer deposition (ALD). For this technique, the relatively high thermal stability and the presence of oxygen containing functional groups on the surface of the carbon spheres are beneficial. Subsequent annealing burned out the template spheres, leaving behind the inverse opal structures. The upper solid TiO₂ layer was removed with argon ion sputtering. The samples were characterized with SEM, Raman spectroscopy, XRD, EDX, UV–Vis diffuse reflectance spectroscopy and their photocatalytic activity was investigated in decomposing organic dyes under UV and visible illumination. A new approach was used to test photocatalysis on the surface by utilizing UV–Vis reflectance and Raman spectroscopy in conjunction.

1. Introduction

Photonic crystals, particularly the inverse opal variants are in the center of many researches because of their favorable and tunable optical properties, which prevent the propagation of light in certain directions with specified frequencies [1,2]. They can be made from a wide variety of dielectric materials, e.g. silicon, silica, titania, ZnO or CdSe, with methods such as sol-gel technique, atomic layer deposition (ALD) or electrodeposition [3–8]. Among these materials, TiO₂ is a widely researched photocatalyst with a band gap of 3.2 eV (anatase form), however, since it absorbs only in the UV range, shifting its absorption to the visible region is preferred. Many approaches are tried for this purpose, such as doping with metal or non-metal elements (e.g. Au, Sn, C or N), using organic dyes for sensitization or making a composite material (for example, with carbon nanotubes or WO₃) [9–17].

Creating inverse opal structure from the TiO₂ offers another method to shift the absorption to visible region without any chemical modification through the slow photon effect. This phenomenon appears due to the interaction of the wave packet reflected by the photonic band gap

with the transmitted wave packet at wavelengths near the gap. Consequently, a stationary wave packet is formed, which possess strongly reduced group velocity, so the lifetime of the photons and the optical path of the light wave increase in the inverse opal. This process helps the light absorption, thus increasing the photocatalytic activity [18–21]. Inverse opals can also be prepared by top-down methods, but bottom-up techniques are more convenient, as they take advantage of the colloidal self-assembly [22–24]. In these approaches, a colloid crystal is prepared from the template spheres, among which the most widely used are polystyrene, poly(methyl methacrylate) and silica, then the gaps between the spheres are filled with the chosen dielectric material. For this purpose, ALD is a highly suitable technique as it ensures homogenous coating of the spheres [25–28]. Finally, the spheres are removed, leaving behind the inverse opal structure. The polymers can be burned out, and silica is usually removed by dissolving it with hydrogen fluoride [29–31].

Our group showed previously that carbon nanospheres (CS) are suitable templates for the atomic layer deposition of TiO₂, because they are thermally stable up to 300 °C in inert atmosphere and have oxygen

* Corresponding author.

E-mail address: laszlobakos@hotmail.com (L.P. Bakos).

<https://doi.org/10.1016/j.apsusc.2019.144443>

Received 1 August 2019; Received in revised form 15 October 2019; Accepted 17 October 2019

Available online 26 October 2019

0169-4332/ © 2019 The Authors. Published by Elsevier B.V. This is an open access article under the CC BY license

(<http://creativecommons.org/licenses/by/4.0/>).

containing functional groups on their surface. By subsequent annealing of the CS-TiO₂ composites, hollow titania shells can be made [32]. In this work, by making an ordered face centered colloidal crystal from the carbon nanospheres, and depositing TiO₂ on it with ALD, inverse opal structures were fabricated. For reference, an inverse opal was prepared from polystyrene nanospheres, which is a widely used conventional template for this purpose. The carbon spheres were tested for thermal stability by thermogravimetry/differential thermal analysis (TG/DTA). The inverse opal samples were investigated with scanning electron microscopy (SEM), Raman spectroscopy, X-ray diffraction (XRD), UV-Vis diffuse reflectance spectroscopy and their photocatalytic activity investigated in decomposing two organic dyes, methyl orange dye in solution, and methylene blue dye dried on the surface of the samples, both under UV and visible light irradiation.

2. Materials and methods

2.1. Preparation of the carbon nanospheres

The carbon nanospheres (CS) were prepared from sucrose solution by a hydrothermal method. The pH was alkaline, set to 11 with NaOH solution. The reaction went for 12 h at 180 °C in an autoclave. The resulting carbon nanospheres were washed with warm distilled water, then with ethanol-water mixture, and afterwards, five times with acetone. The resulting black powder was dried overnight at 70 °C. The average diameter of the spheres was 458 nm, with a standard deviation of 80 nm, which parameters were calculated from SEM images.

2.2. Preparation of the colloidal crystal

For reference, inverse opals were prepared from polystyrene spheres (PS) as well (10 wt% in water, 300 nm diameter, with a standard deviation of 40 nm), which was bought from Sigma-Aldrich. The synthesis process was the same for both CS and PS. It started with making a 0.3 wt% suspension in distilled water, which was placed in an ultrasonic bath for 2 h to separate the aggregated nanospheres. The substrates were microscope slides, cleaned with soap, ethanol, then held 1 h in piranha solution (mixture of cc. H₂SO₄ and 30% H₂O₂, in 3:1 ratio) to remove any organic remnants and make the surface hydrophilic. After that, the glass slides were placed vertically in 5 ml suspensions of the CS and PS. They were put in a furnace at 50 °C for 14 h, so the colloidal crystal could form during the evaporation of the water through colloidal self-assembly, and were finally heated to 80 °C for 1.5 h.

2.3. Atomic layer deposition

The CS and PS colloidal crystals on the glass substrates were put in a Beneq TFS-200-186 flow ALD machine. The atomic layer deposition (ALD) of the TiO₂ was performed at 50 °C, the pressure was 1 mbar in the reaction chamber. One deposition cycle was 0.3 s pulse of TiCl₄ precursor, 3 s nitrogen purge, 0.3 s pulse of H₂O and 3 s nitrogen purge, and this cycle was repeated for 700 times. A clean glass substrate was placed alongside the samples during the ALD, and the thickness of the deposited oxide layer was measured on it by profilometry to be 55 nm.

2.4. Obtaining the inverse opal

The nanosphere-TiO₂ composites were annealed in air in a Nabertherm L9/11/B410 furnace, i.e. heated to 500 °C under 4 h, and stayed at that temperature for 2 h. This process burnt out the CS and PS, leaving behind the TiO₂ inverse opal structure. Finally, the inverse opals were sputtered for 100 min at 20 A current with argon ions in a Leybold Heraeus instrument to remove upper solid TiO₂ layer to get the underlying inverse opal structure.

2.5. Characterization

TG/DTA measurements of the carbon spheres were made in a TA Instruments SDT 2960 machine, with a heating rate of 10 °C/min until 900 °C, under 130 cm³/min gas flow. The measurement under nitrogen flow simulated the environment in the ALD reactor, and the data in air gave information about the annealing process.

For the SEM images, a LEO 1540 XB scanning electron microscope was used, in high vacuum mode with a secondary electron detector. Adhesive carbon tapes were used to fix the samples on a copper sample holder. To prevent the carbon and polystyrene nanosphere opals from charging, they were sputtered with an Au/Pd layer, which step was unnecessary for the TiO₂ inverse opals.

EDX spectra were measured on a JEOL JSM-5500LV scanning electron microscope, and three EDX measurements were averaged for each sample.

Raman spectra were taken on a Jobin Yvon Labram Raman spectroscope equipped with an Olympus BX41 microscope, using green (532 nm) Nd-YAG laser. The measured range of the Raman shift was between 100 and 1800 cm⁻¹.

X-ray diffractograms were made on a PANalytical X'Pert Pro MPD X-ray diffractometer using Cu K α radiation, the measurement range was 5–65°.

To get the UV-Vis diffuse reflectance spectra, a JASCO V-750 UV-VIS spectrophotometer with an integrating sphere was utilized with BaSO₄ reference material, between 300 and 800 nm. The band gap was determined with Kubelka-Munk theory from Tauc plot [33].

Photocatalytic activity was tested in two different setups (Fig. S1A–B). In the first one, the samples were immersed in 10 cm³ methyl orange solution with a concentration of 4×10^{-5} M. The solution was stirred for one hour so that the adsorption equilibrium could occur, after which the irradiation started. For the experiments involving methylene blue, a 25 μ L droplet of a 0.001 M solution was put on the surface of the samples and dried for 1 h before the illumination. The samples were tested in both cases with UV and visible light lamps as well, the spectra of the lamps are on Fig. S2. Three 18 W fluorescent lamp was used in each experiment, stacked on each other, and the sample was in front of the middle lamp at a distance of 5 cm. The decomposition of the organic dyes was followed by an Avantes AvaSpec-2048 fiber optic spectrometer, with an AvaLight-DHS light source, using its own AvaSoft software. For the methyl orange measurements, every half hour 3 cm³ was taken from solution, whose absorbance was measured in a quartz cuvette, and was put back in for further photocatalysis. The decomposition of the methyl orange was followed by the decrease in the relative absorbance (A/A_0) of its most intensive peak at 464 nm. For the methylene blue experiments, the absorbance was measured in reflectance mode with the same spectrometer, where the bare inverse opal structure was the background, and spectra were taken before and after the 4 h irradiation. The methylene blue peaks maximum were at different positions, on the inverse opal made with carbon spheres (CSIO), it was at 668 nm, and in case of the inverse opal from polystyrene spheres (PSIO), it was at 530 nm. The peaks were integrated from 400 to 770 nm for the CSIO, and from 420 to 700 nm for the PSIO. This measurement was followed by Raman spectroscopy as well, and the spectra were normalized for the most intensive peak of the sample, which was the 146 cm⁻¹ peak of the anatase TiO₂. From the many peaks of the methylene blue, the intensity of its most intensive peak at 1630 cm⁻¹ was examined, and the peak area was integrated from 1570 cm⁻¹ to 1670 cm⁻¹.

3. Results and discussion

Thermogravimetry data on Fig. 1 show that the carbon spheres (CS) were stable in nitrogen atmosphere until around 300 °C, when they started to decompose, leaving behind half of the mass at 900 °C. This ensured their stability during the ALD and enables higher temperature

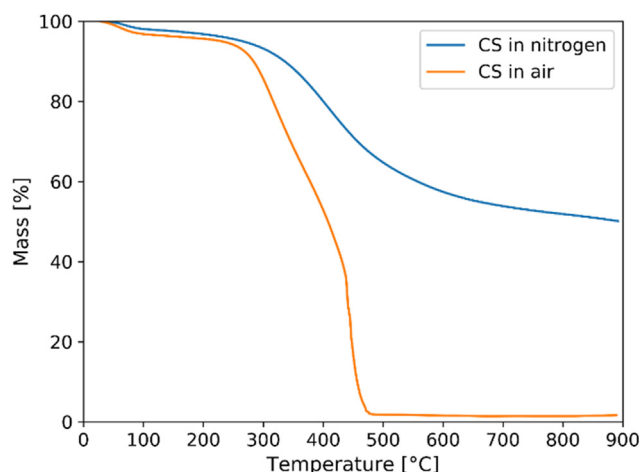


Fig. 1. TG analysis of the carbon spheres.

depositions in the future. In air, they fully burnt out at 500 °C, so the template CS could be removed by annealing to this temperature. The decomposition was endothermic in nitrogen, and fiercely exothermic in air (DTA curves on Figs. S3–4). According to literature data, polystyrene begins to flow around 100 °C (its glass transition temperature), so the chosen ALD temperature of 50 °C was necessary to avoid the deformation of the template, considering the highly exothermic reaction of TiCl_4 with water when the TiO_2 forms [34].

SEM pictures (Fig. 2a and c) reveal the successful synthesis of the face centered cubic colloidal crystals (opals) from CS and PS. The

Table 1

Composition of the inverse opals from EDX spectra.

| Element | O | Na | Al | Si | Cl | Ca | Ti |
|---------|----------|-----|-----|-----|-----|-----|------|
| | atomic % | | | | | | |
| CSIO | 65.9 | 3.9 | 1.1 | 8.0 | 0.7 | 0.8 | 19.6 |
| PSIO | 65.7 | 0.7 | 1.1 | 8.5 | 0.2 | 1.0 | 22.8 |

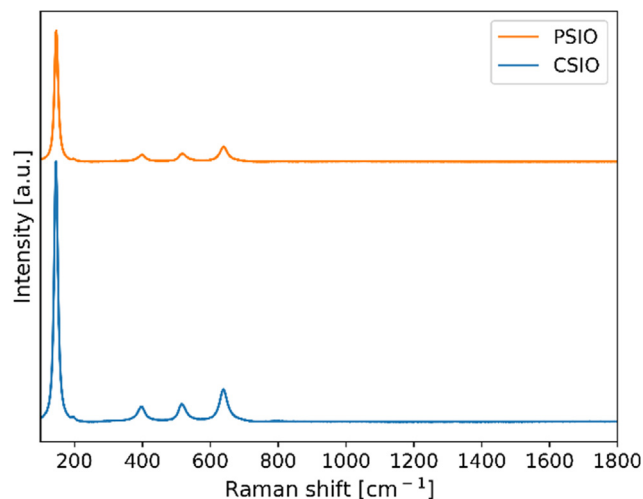


Fig. 3. Raman spectra of the titania inverse opals.

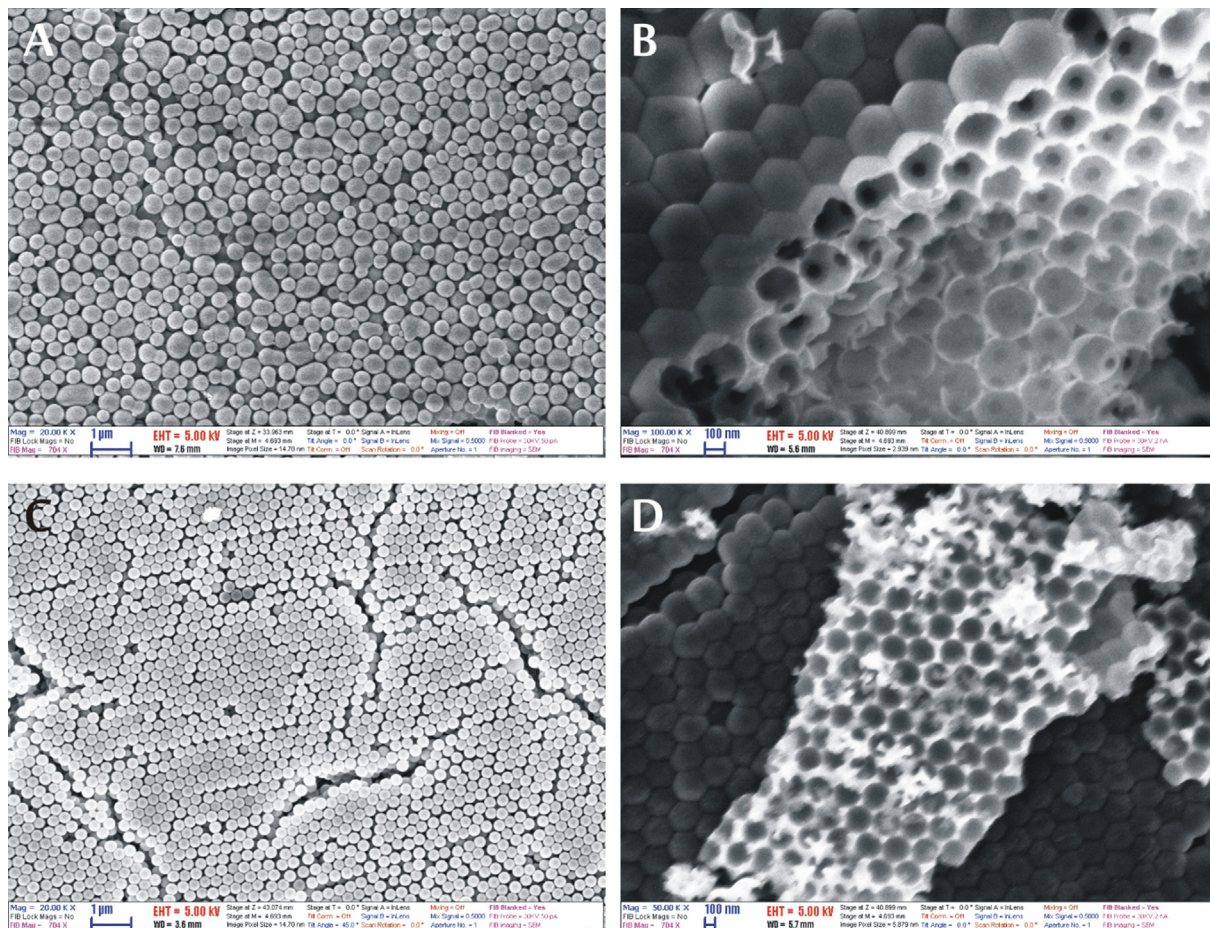


Fig. 2. SEM pictures of the samples (A: carbon sphere opal, B: TiO_2 inverse opal from CS, C: polystyrene sphere opal, D: TiO_2 inverse opal from PS).

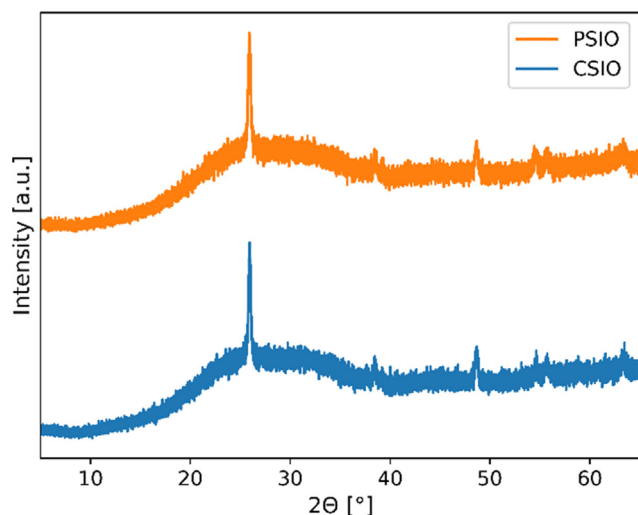


Fig. 4. XRD diffractograms of the TiO₂ inverse opals.

polystyrene spheres had a narrower size distribution (RSD: 13.3%) compared to the carbon spheres (RSD: 17.5%), and the spheres are more identical, so the PS opal is slightly more ordered than the CS opal. In Fig. 2b and d, the titania inverse opals with their hollow structure and interconnected spheres are visible.

EDX results in Table 1 show the approximate composition of the inverse opals. Because of their hollow structure, signals from the glass substrate (Na, Al, Si and Ca) are also detectable beside the Ti and O from the TiO₂. The small amount of Cl is residue from the ALD process, as TiCl₄ precursor was used.

Raman spectra in Fig. 3 shows that both samples were composed of pure anatase TiO₂. Its characteristic peaks are at 146, 400, 507 and 640 cm⁻¹ [35]. The templates were completely removed with annealing from the structure, as no D and G peaks of the carbon are visible [32].

XRD diffractograms (Fig. 4) confirmed the Raman results, the samples were pure anatase (ICDD card number: 01-075-2546). The amorphous background is due to the glass microscope slide substrates.

For the inverse opals were white, non-transparent coatings on the microscope slide substrates, diffuse reflectance spectra were taken from them (Fig. 5). The photonic band gap (PBG) of the inverse opal structure is clearly present, which is the decrease in the absorbance above the absorption edge of TiO₂ (380 nm). The PSIO has its PBG at around 420 nm, while the CSIO has it at 550 nm, for the spheres were greater

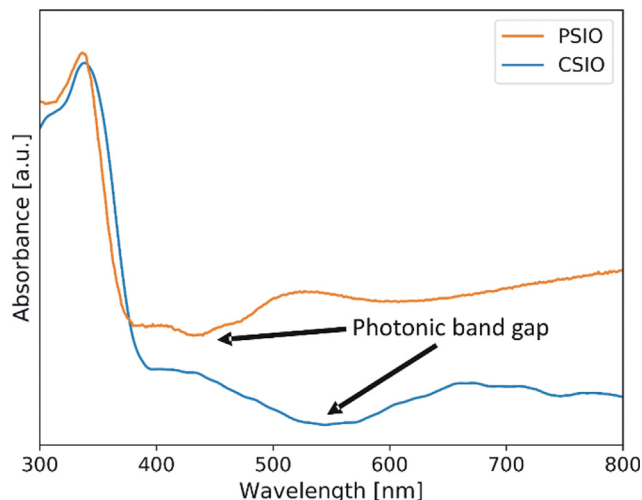


Fig. 5. Diffuse reflectance spectra of the inverse opals.

on average. The absorbance increased at the blue and red edges of the PBGs thus visible light was absorbed, which phenomenon is not shown in case of anatase TiO₂ powder [36]. Using different sized template spheres, the size of the air pockets in inverse opals can be changed. This way, the photonic band gap can be tuned, as the diameter of the templates determines the position of the band gap, and sharper peak can be achieved with more identical spheres. For idealized cases, Bragg theory can be used to calculate the exact position of the stop band [37]. In our case, increase in the visible absorption was achieved. The calculated band gap of the bulk TiO₂ (Fig. S5A–B) was around 3.20 eV, for both samples, as it is the expected literature value for anatase TiO₂ [38].

The results of the photocatalytic decomposition of methyl orange dye in solution are shown in Fig. S6 and Table S1. Under visible light, no decomposition was detected without inverse opals, and the activity of the samples was very low. Under UV light, there was measurable photolysis of the methyl orange, and the activity of the samples was greater. In all cases, only a little decomposition of the dye was measured, because the surface area of the samples was low compared to the amount of solution, so another approach was needed.

For this reason, methylene blue was dried on the inverse opals, and the decomposition on the surface was followed with UV–Vis reflectance spectroscopy (Fig. 6). While according to the Raman and XRD measurements, the samples are identical regarding their composition, the reflectance spectra of the methylene blue differs. In case of all samples, the methylene blue decomposed, even under visible light. This measurement was further followed by Raman spectroscopy (Figs. 7 and 8), with similar result as it can be seen in Table 2. In case of the PSIO under visible light irradiation, it showed better performance when investigated with Raman spectroscopy, 58.5% decrease, while with UV–Vis reflectance spectroscopy, it was only 27.5%. This discrepancy may be caused by surface irregularities on the sample. This technique is a more sensitive way to measure the photocatalytic properties of inverse opals structures, compared to wet photocatalysis in solution. For a non-transparent film photocatalyst, e.g. to use in air purification, this can be a more suitable method to evaluate the photocatalytic activity.

4. Conclusions

In this study, we used carbon nanospheres to fabricate inverse opal photonic crystals, which were never used before as templates for this purpose to the best of our knowledge. For reference, inverse opals were made from conventional polystyrene nanospheres. The higher temperature tolerance and surface functional groups of the carbon spheres make them more suitable templates for atomic layer deposition than polymer spheres and are easier to remove than silica spheres. Face-centered cubic colloid crystals were prepared from the templates by taking advantage of colloidal self-assembly, and atomic layer deposition was utilized to fill the gaps between the spheres with titania. After annealing and sputtering with argon ions, SEM images revealed the hollow inverse opal structure with interconnected spheres. The bulk material was pure anatase TiO₂, as proved by Raman spectroscopy and XRD measurements, and no carbon remained after annealing. UV–Vis diffused reflectance spectroscopy confirmed the presence of the visible photonic band gap. The CSIO had the photonic band gap at a higher wavelength, and was less defined than for the PSIO, because of the larger average diameter and wider size distribution of the carbon spheres. The samples possess photocatalytic activity under UV and visible light in decomposing organic dyes, while bulk TiO₂ only works under UV light, so this behavior can be attributed to the presence of the photonic band gap due to the inverse opal structure. A new method was developed to test photocatalysis on the surface in case of the methylene blue dye, by utilizing both UV–Vis reflectance and Raman spectroscopy, which can be a better way to evaluate activity for non-transparent films, like inverse opals, as it is a more sensitive technique compared to measuring in solution.

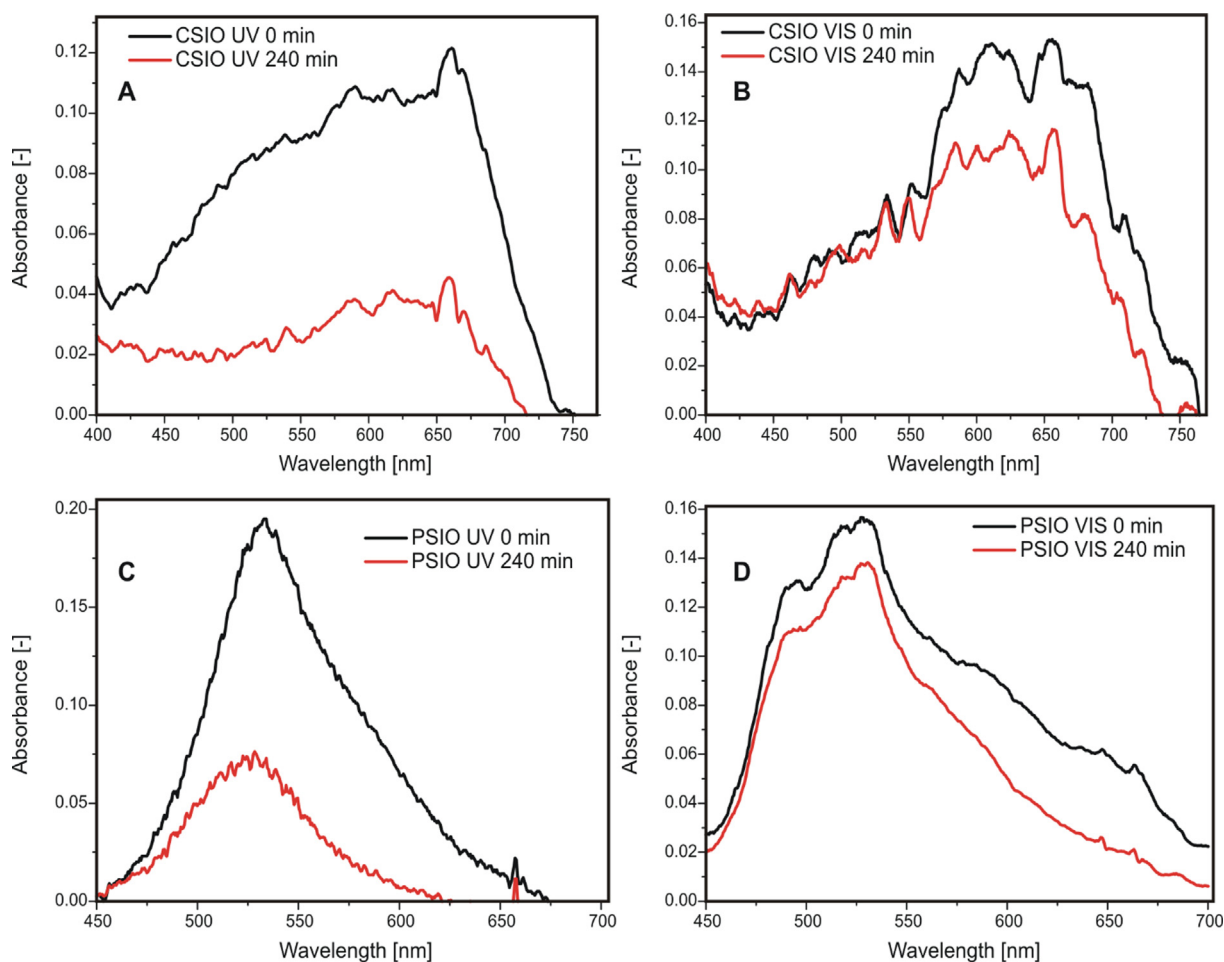


Fig. 6. Photocatalytic decomposition of methylene blue dried on the samples: on the surface of CSIO under UV (A) and visible (B), on the PSIO under UV (C) and visible (D) light.

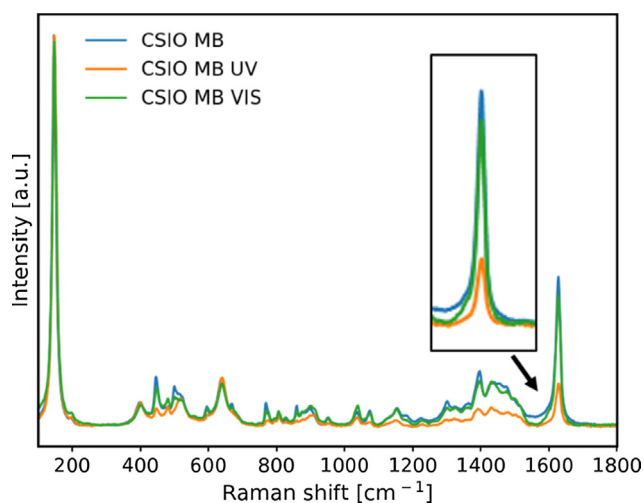


Fig. 7. Raman spectra of the methylene blue dried on the surface of the CSIO before after 4 h irradiations.

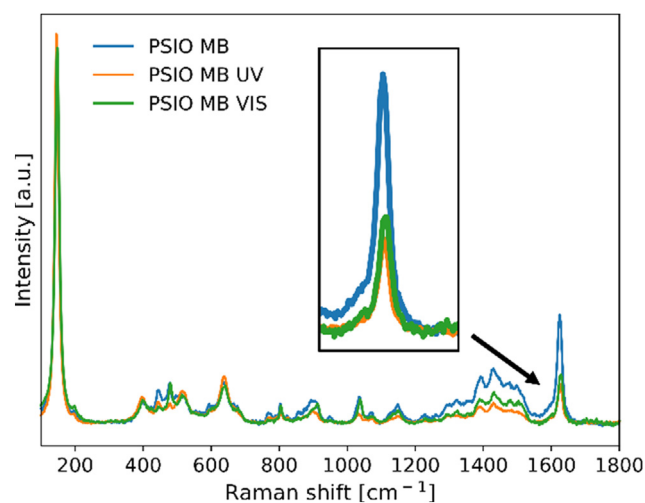


Fig. 8. Raman spectra of the methylene blue dried on the surface of the PSIO before and after 4 h irradiations.

Declaration of Competing Interest

The authors declare that they have no known competing financial interests or personal relationships that could have appeared to influence the work reported in this paper.

Acknowledgments

I. M. Szilágyi thanks for a János Bolyai Research Fellowship of the Hungarian Academy of Sciences. The ÚNKP-18-4-BME-238 New National Excellence Program of the Ministry of Human Capacities, Hungary. A GINOP-2.2.1-15-2017-00084, an NRDI K 124212, an NRDI TNN_16 123631 and an NRDI K 128266 grants are acknowledged. The

Table 2

Results of the photocatalytic decomposition of the methylene blue as decrease in peak areas according to UV–Vis reflectance and Raman spectroscopy.

| Sample | UV–VIS [%] | Raman [%] |
|----------|------------|-----------|
| CSIO UV | 70.3 | 72.7 |
| PSIO UV | 69.6 | 67.6 |
| CSIO VIS | 23.6 | 19.9 |
| PSIO VIS | 27.5 | 58.5 |

work performed within project VEKOP-2.3.2-16-2017-00013 was supported by the European Union and the State of Hungary, co-financed by the European Regional Development Fund. The research reported in this paper was supported by the Higher Education Institutional Excellence Program of the Ministry of Human Capacities in the frame of Nanotechnology and Materials Science research area of Budapest University of Technology (BME FIKP-NAT) and the Energetics thematic programme of the University of Debrecen (NKFIH-1150-6/2019). The authors are thankful for Dr. Balázs Réti (Department of Applied and Environmental Chemistry, University of Szeged, Szeged, Hungary) for the carbon nanospheres, Tamás Igricz (Department of Organic Chemistry and Technology, Budapest University of Technology and Economics, Budapest, Hungary) for the Raman measurements and Dr. Ágnes Szegedi (Green chemistry Research Group, Institute of Materials and Environmental Chemistry, Hungarian Academy of Sciences, Budapest, Hungary) for the UV–Vis diffuse reflectance measurements.

Appendix A. Supplementary material

Supplementary data to this article can be found online at <https://doi.org/10.1016/j.apsusc.2019.144443>.

References

- [1] E. Armstrong, C. O'Dwyer, Artificial opal photonic crystals and inverse opal structures – fundamentals and applications from optics to energy storage, *J. Mater. Chem. C* 3 (2015) 6109–6143, <https://doi.org/10.1039/C5TC01083G>.
- [2] J.D. Joannopoulos, S.G. Johnson, J.N. Winn, R.D. Meade, *Photonic Crystals: Molding the Flow of Light*, Princeton University Press, 2008 <https://doi.org/10.1088/1751-8113/44/8/085201>.
- [3] B. Shao, Z. Yang, Y. Wang, J. Li, J. Yang, J. Qiu, et al., Coupling of Ag nanoparticle with inverse opal photonic crystals as a novel strategy for upconversion emission enhancement of NaYF₄: Yb³⁺, Er³⁺ nanoparticles, *ACS Appl. Mater. Interfaces* 7 (2015) 25211–25218, <https://doi.org/10.1021/acsami.5b06817>.
- [4] A. Blanco, E. Chomski, S. Grubtchak, M. Ibsate, S. John, S.W. Leonard, et al., Large-scale synthesis of a silicon photonic crystal with a complete three-dimensional bandgap near 1.5 micrometres, *Nature* 405 (2000) 437–440, <https://doi.org/10.1038/35013024>.
- [5] J. Liu, C. Sun, M. Fu, J. Long, D. He, Y. Wang, Enhanced photochemical catalysis of TiO₂ inverse opals by modification with ZnO or Fe₂O₃ using ALD and the hydrothermal method, *Mater. Res. Exp.* 5 (2018) 025509, <https://doi.org/10.1088/2053-1591/aaabe9>.
- [6] J. Xu, B. Yang, Z. Fu, M. Wen, Y. Zhao, Synthesis and photocatalytic property of ZnO/TiO₂ inverse opals films with controllable composition and topology, *Chinese J. Chem. Phys.* 25 (2012) 235–241, <https://doi.org/10.1088/1674-0068/25/02/235-241>.
- [7] P.V. Braun, P. Wiltzius, Electrochemically grown photonic crystals, *Curr. Opin. Colloid Interface Sci.* 7 (2002) 116–123, [https://doi.org/10.1016/S1359-0294\(02\)00009-2](https://doi.org/10.1016/S1359-0294(02)00009-2).
- [8] B. Hatton, L. Mishchenko, S. Davis, K.H. Sandhage, J. Aizenberg, Assembly of large-area, highly ordered, crack-free inverse opal films, *Proc. Natl. Acad. Sci.* 107 (2010) 10354–10359, <https://doi.org/10.1073/pnas.1000954107>.
- [9] X.Z. Li, F.B. Li, Study of Au/Au 3+ -TiO₂ photocatalysts toward visible photo-oxidation for water and wastewater treatment, *Environ. Sci. Technol.* 35 (2001) 2381–2387, <https://doi.org/10.1021/es001752w>.
- [10] Y. Cao, W. Yang, W. Zhang, G. Liu, P. Yue, Improved photocatalytic activity of Sn⁴⁺ doped TiO₂ nanoparticulate films prepared by plasma-enhanced chemical vapor deposition, *New J. Chem.* 28 (2004) 218, <https://doi.org/10.1039/b306845e>.
- [11] R. Asahi, Visible-light photocatalysis in nitrogen-doped titanium oxides, *Science* (80-.) 293 (2001) 269–271, <https://doi.org/10.1126/science.1061051>.
- [12] N.R. Khalid, A. Majid, M.B. Tahir, N.A. Niaz, S. Khalid, Carbonaceous-TiO₂ nanomaterials for photocatalytic degradation of pollutants: a review, *Ceram. Int.* 43 (2017) 14552–14571, <https://doi.org/10.1016/j.ceramint.2017.08.143>.
- [13] M. Zhang, C. Chen, W. Ma, J. Zhao, Visible-light-induced aerobic oxidation of alcohols in a coupled photocatalytic system of dye-sensitized TiO₂ and TEMPO, *Angew. Chemie Int. Ed.* 47 (2008) 9730–9733, <https://doi.org/10.1002/anie.200803630>.
- [14] S.W. Verbruggen, TiO₂ photocatalysis for the degradation of pollutants in gas phase: From morphological design to plasmonic enhancement, *J. Photochem. Photobiol. C Photochem. Rev.* 24 (2015) 64–82, <https://doi.org/10.1016/j.jphotochemrev.2015.07.001>.
- [15] T. Jiang, L. Zhang, M. Ji, Q. Wang, Q. Zhao, X. Fu, et al., Carbon nanotubes/TiO₂ nanotubes composite photocatalysts for efficient degradation of methyl orange dye, *Particuology* 11 (2013) 737–742.
- [16] I.M. Szilágyi, E. Santala, M. Heikkilä, V. Pore, M. Kemell, T. Nikitin, et al., Photocatalytic properties of WO₃/TiO₂ core/shell nanofibers prepared by electrospinning and atomic layer deposition, *Chem. Vap. Depos.* 19 (2013) 149–155, <https://doi.org/10.1002/cvde.201207037>.
- [17] E. Albert, P.A. Albouy, A. Ayral, P. Basa, G. Csik, N. Nagy, et al., Antibacterial properties of Ag–TiO₂ composite sol–gel coatings, *RSC Adv.* 5 (2015) 59070–59081, <https://doi.org/10.1039/C5RA05990A>.
- [18] J.L.L. Chen, G. Von Freymann, S.Y. Choi, V. Kitaev, G.A. Ozin, Amplified photochemistry with slow photons, *Adv. Mater.* 18 (2006) 1915–1919, <https://doi.org/10.1002/adma.200600588>.
- [19] J. Liu, H. Zhao, M. Wu, B. Van der Schueren, Y. Li, O. Deparis, et al., Slow photons for photocatalysis and photovoltaics, *Adv. Mater.* 29 (2017) 1–21, <https://doi.org/10.1002/adma.201605349>.
- [20] X. Zheng, S. Meng, J. Chen, J. Wang, J. Xian, Y. Shao, et al., Titanium dioxide photonic crystals with enhanced photocatalytic activity: matching photonic band gaps of TiO₂ to the absorption peaks of dyes, *J. Phys. Chem. C* 117 (2013) 21263–21273, <https://doi.org/10.1021/jp404519j>.
- [21] M. Curti, C.B. Mendive, M.A. Grela, D.W. Bahnemann, Stopband tuning of TiO₂ inverse opals for slow photon absorption, *Mater. Res. Bull.* 91 (2017) 155–165, <https://doi.org/10.1016/j.materresbull.2017.03.061>.
- [22] J. Zhang, Z. Sun, B. Yang, Self-assembly of photonic crystals from polymer colloids, *Curr. Opin. Colloid Interface Sci.* 14 (2009) 103–114, <https://doi.org/10.1016/j.cocis.2008.09.001>.
- [23] P. Jiang, J.F. Bertone, K.S. Hwang, V.L. Colvin, Single-crystal colloidal multilayers of controlled thickness, *Chem. Mater.* 11 (1999) 2132–2140, <https://doi.org/10.1021/cm990080+>.
- [24] Z. Zhou, X.S. Zhao, Flow-controlled vertical deposition method for the fabrication of photonic crystals, *Langmuir* 20 (2004) 1524–1526, <https://doi.org/10.1021/la035686y>.
- [25] C. Marichy, N. Pinna, Carbon-nanostructures coated/decorated by atomic layer deposition: growth and applications, *Coord. Chem. Rev.* 257 (2013) 3232–3253, <https://doi.org/10.1016/j.ccr.2013.08.007>.
- [26] S.M. George, Atomic layer deposition: an overview, *Chem. Rev.* 110 (2010) 111–131, <https://doi.org/10.1021/cr900056b>.
- [27] I. Alessandri, M. Zucca, M. Ferroni, E. Bontempi, L.E. Depero, Tailoring the pore size and architecture of CeO₂/TiO₂ core/shell inverse opals by atomic layer deposition, *Small* 5 (2009) 336–340, <https://doi.org/10.1002/smll.200801249>.
- [28] J.S. King, E. Graugnard, C.J. Summers, TiO₂ inverse opals fabricated using low-temperature atomic layer deposition, *Adv. Mater.* 17 (2005) 1010–1013, <https://doi.org/10.1002/adma.200400648>.
- [29] Z. Cai, Z. Xiong, X. Lu, J. Teng, In situ gold-loaded titania photonic crystals with enhanced photocatalytic activity, *J. Mater. Chem. A* 2 (2014) 545–553, <https://doi.org/10.1039/c3ta13878j>.
- [30] G.I.N. Waterhouse, M.R. Waterland, Opal and inverse opal photonic crystals: fabrication and characterization, *Polyhedron* 26 (2007) 356–368, <https://doi.org/10.1016/j.poly.2006.06.024>.
- [31] T. Kohoutek, J. Orava, T. Sawada, H. Fudouzi, Inverse opal photonic crystal of chalcogenide glass by solution processing, *J. Colloid Interface Sci.* 353 (2011) 454–458, <https://doi.org/10.1016/j.jcis.2010.10.011>.
- [32] N. Justh, L.P. Bakos, K. Hernádi, G. Kiss, B. Réti, Z. Erdélyi, et al., Photocatalytic hollow TiO₂ and ZnO nanospheres prepared by atomic layer deposition, *Sci. Rep.* 7 (2017) 4337, <https://doi.org/10.1038/s41598-017-04090-0>.
- [33] J. Tauc, T.A. Scott, The optical properties of solids, *Phys. Today* 20 (1967) 105–107, <https://doi.org/10.1063/1.3033945>.
- [34] J. Rieger, The glass transition temperature of polystyrene, *J. Therm. Anal.* 46 (1996) 965–972, <https://doi.org/10.1007/BF01983614>.
- [35] M.J. Šćepanović, M. Grujić-Brojin, Z.D. Dohčević-Mitrović, Z.V. Popović, Characterization of anatase TiO₂ nanopowder by variable-temperature Raman spectroscopy, *Sci. Sinter.* 41 (2009) 67–73, <https://doi.org/10.2298/SOS0901067S>.
- [36] L.-L. Tan, W.-J. Ong, S.-P. Chai, A. Mohamed, Reduced graphene oxide-TiO₂ nanocomposite as a promising visible-light-active photocatalyst for the conversion of carbon dioxide, *Nanos. Res. Lett.* 8 (2013) 465, <https://doi.org/10.1186/1556-276X-8-465>.
- [37] R.C. Schroden, M. Al-Daous, C.F. Blanford, A. Stein, Optical properties of inverse opal photonic crystals, *Chem. Mater.* 14 (2002) 3305–3315, <https://doi.org/10.1021/cm020100z>.
- [38] J. Zhang, P. Zhou, J. Liu, J. Yu, New understanding of the difference of photocatalytic activity among anatase, rutile and brookite TiO₂, *Phys. Chem. Chem. Phys.* 16 (2014) 20382–20386, <https://doi.org/10.1039/c4cp02201g>.